Speeding up and boosting tsunami warning in Chile

Mauricio Fuentes[1], Sebastian Arriola[2], Sebastian Riquelme[2], and Bertrand Delouis[3]

[1]Department of Geophysics, Faculty of Physical and Mathematical Sciences, University of Chile
[2]National Seismological Center, Faculty of Physical and Mathematical Sciences, University of Chile
[3]Géoazur, Université de Nice Sophia Antipolis, Observatoire de la Côte d'Azur

Correspondence: Mauricio Fuentes (mauricio@dgf.uchile.cl)

Abstract. Chile host a great tsunamigenic potential along its coast, even with the large earthquakes occurred during the last decade, there is still a large amount of seismic energy to release. This permanent feature and the fact that the distance between the trench and the coast is just 100 km creates a difficult environment to do real time tsunami forecast. In Chile tsunami warnings are based on reports of the seismic events (hypocenter and magnitude) and a database of precomputed tsunami scenarios. However, because yet there is no answer to image the finite fault model within first minutes (before the first tsunami wave arrival), the precomputed scenarios consider uniform slip distributions. Here, we propose a scheme of processes to fill the gaps in-between blind zones due to waiting of demanding computational stages. The linear shallow water equations are solved to obtain a rapid estimation of the run-up distribution in the near field. Our results show that this linear method captures most of the complexity of the run-up heights in terms of shape and amplitude when compared with a fully non-linear tsunami code. Also, the run-up distribution is obtained in quasi real-time as soon as the seismic finite fault model is produced.

Copyright statement. TEXT

1 Introduction

For decades, coastal-exposed countries have been working on tsunami warning systems (Doi, 2003; Wächter et al., 2012). Due to the tsunami source process, most of them are attributed to large subduction earthquake or to landslides, then real-time forecast is out of reach. Regular earthquakes follow a scaling law in terms of its released energy (seismic moment) and its duration (Ide et al, 2007). For instance, a regular M_w 8.5 can last for $\approx$ 2 minutes, whereas tsunami generation is considered quasi-instantaneous after the source time. This implies that a robust tsunami warning system must be related to different monitoring systems of potential triggers (earthquakes, volcanoes, among others). In the case of tsunamis generated by subduction earthquakes, to detect and to characterize the seismic source is crucial. Nowadays, the W-phase method is the preferred for accounting large earthquakes in Chile (Riquelme et al, 2016, 2018). A first moment tensor solution can be obtained in 5 minutes. However, it is well-known that tsunami heights are highly sensitive to the spatial slip distribution of the seismic source (Geist, 2002; Ruiz et al., 2015). Even having a finite fault model, the simulation of the tsunami propagation can take several hours depending on the desired level of resolution. This is the reason why many of the current warning systems
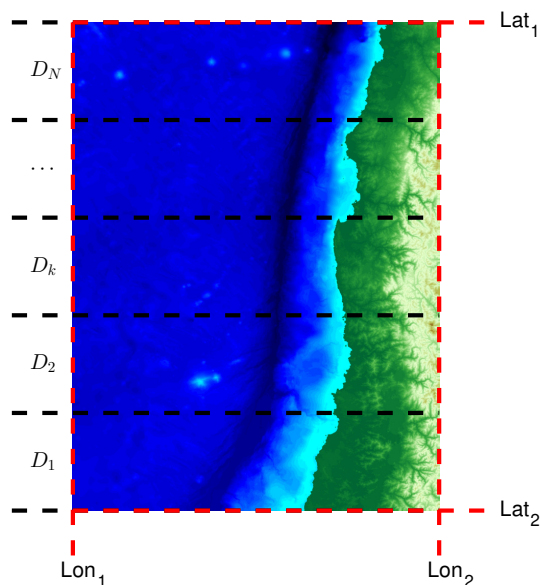
are based on precomputed scenarios. Chile and Japan use this methodology for that purpose (https://www.jma.go.jp/jma/en/News/lists/tsunamisystem2006mar.pdf). However, this methodology ignores the complexity of the seismic source resolving for uniform slip models only. In this work we propose a methodology specific for near-field tsunamis triggered by earthquakes that complements information to the operating monitoring systems and helps to make decisions during and after the emergency alert.

5 ## 2 Methodology

This problem is separated in three parts. The determination of a seismic source model, the generation of an initial condition and the corresponding tsunami simulation. We define a computation domain around the earthquake source and the coastal areas in the near field. The bathymetric data used is the SRTM15 with 15 arcsec of resolution, based on the STM30 (Becker et al., 2009).

10   The idea here is to trade off accuracy for rapidness. In a near field earthquake tsunami context we care about the maximum inundation place, the extension of the inundation until decreases to 0.5 to 1 m, and the average run-up. This model is not trying to be as accurate as possible and to determine a detailed inundation map but what intends to do is to give an idea of the main area that is going to be affected using the W-phase CMT, which is currently one of the fastest methodology to characterize large earthquake parameters in real time (Kanamori and Rivera, 2008).

Figure 1. Sketch of the partition of the computation domain for parallel running.

Natural Hazards
and Earth System
Sciences
Discussions

Open Access

EGU

2.1 The slip distribution model

Once an earthquake is firstly described by the W-phase solution, we use an elliptical slip distribution (Dmowska and Rice, 1986) over a region determined with the scaling laws obtained by Blaser et al. (2010). This serves as a first estimation while seismic waves are still traveling, and subsequent finite fault solutions are computed. Thus, we can model the near field tsunami

5   for every finite fault model update.

2.2 The tsunami initial condition

Despite there are evidences of influence in the tsunami generation process with the source time components, for quickness purposes, we model static seafloor deformation induced by a non-uniform slip distribution including the horizontal components, as suggested in Tanioka and Satake (1996). This is obtained with that Okada's equations (Okada, 1985).

10   ## 2.3 The tsunami modeling

The last part of this methodology is to obtain the tsunami heights along the coast. Usually, tsunami modeling involves complex codes to solve the fully coupled non-linear shallow water equations. Depending on the domain size and resolution, a full tsunami run can take several hours, which make real-time forecast impossible. To overcome this limitation, we solve the linear shallow water equations with a forward finite difference scheme. The propagation inside the domain is governed by the second

15   order PDE with initial conditions:

$$\eta_{tt} - g\nabla\left(h\nabla\eta\right) = 0$$
$$\eta(x,y,0) = \eta_0(x,y) \qquad\qquad (1)$$
$$\eta_t(x,y,0) = 0$$

where $\eta(x,y,t)$ is the water surface, g is the gravity acceleration, $h(x,y)$ is the bathymetry and $\eta_0(x,y)$ is the initial condition. In the open boundaries, we set a radiation condition (Reid and Bodine, 1968), whereas in the solid boundaries (coasts) we impose full reflection in a vertical wall placed at an isobath of 100 m, before to reach the non-linear zone. Here, Neumann

20   boundary condition is applied: $\frac{\partial\eta}{\partial\hat{n}}$ where $\hat{n}$ denotes the exterior unit normal vector.

The linear method (hereafter, LM) allows to obtain a quicker estimation than a full tsunami code since second-order terms are neglected but keeping the same main features. Also, this approach does not require to compute the velocity field, making the computation programs even faster.

Each simulation is compared with a fully linear water shallow water equation propagation. We select the JAGURS code

25   (Baba et al., 2014) which runs in Fortran90 in a parallel array with OpenMP and OpenMP + MPI. This code is based in the classical finite difference method of Satake (2002). For each scenario, the tsunami is propagated during two hours of tsunami-time, to obtain the main features of the runup distributions, despite the fact that later amplification of edge waves and resonances can occur.

3 Tests and results

For evaluating the performance of this simple approach, we have modeled nearly all of the great tsunamis in the last two decades. Most of them were already tested with an analytical approach in (Riquelme et al, 2015). The details of the propagation and runup distribution of the 12 events tested are exhibited in the supporting information.

5   For these examples we used the finite fault models obtained from USGS (Hayes, 2017), because they have proven to be operational and robust for real time operations in a global context monitoring.

     All the computations were performed in a Dell Precision 7920, with two Intel Xeon Gold 6136 processor, 12 physical core each, for a total of 24 physical core, 2 threads each. For each time iteration, the domain is divided in 48 subdomains that are computed in different threads, for a parallel array (Fig. 1).

10   To compute the tsunami initial condition, the Okada's equations were implemented in C-language using threading, as well as the finite difference scheme for the LM. The C-code uses pthread library. With this tool, a data struct containing a pthread_t was defined, and then a routine that send every grid's subdomain to each different core's thread for computation. This method is such reliable as any other linear scheme method, because it solves the same equations. The only significant difference is the threads distribution for time optimization. When a thread finishes, it computes for a certain time step and it joins with the

15 others in order to avoid miscomputations. For instance, with the used machine, in a regular grid of 4 million points with a FFM of 300 subfaults, the vertical and horizontal seafloor displacements can be calculated almost instantly (less than 5 seconds) and two hours of tsunami propagation for 2011 Tohoku, Japan earthquake can be solved in 60 seconds.

3.1 Examples

All the earthquakes presented here, have produced tsunamis. The range of magnitude varies from 7.7 to 9.1. They occurred

20 in different subduction zones around the world. The largest ones are Tohoku in Japan and Maule in Chile. All of them show a thrust mechanism except for the Samoa event in 2009 which is a normal event. There are a few tsunami earthquakes in this section such as the 1992 Mw 7.7 Nicaragua Earthquake, The 2006 Mw 7.6 Java earthquake. The extension of the earthquakes varies from $L = 150$ km to $L = 500$ km, the range of peak displacement at the source varies from 3 m to 40 m. Therefore, we have tested as many earthquakes and as many source features as possible for this study.

25   1. The 1992 Mw 7.7 Nicaragua Tsunami Earthquake

     2. The 2001 Mw 8.4 Southern Perú Earthquake

     3. The 2003 Mw 8.3 Hokkaido Earthquake

     4. The 2006 Mw 7.6 Java Earthquake

     5. The 2007 Mw 8.1 Solomon Islands Earthquake

30   6. The 2007 Mw 8.0 Pisco Earthquake

Table 1. Correlation of the runup distribution between the linear solution and the JAGURS code.

Event	FFM lon	FFM lat	Elliptic lon	Elliptic lat
1992 Nicaragua	0.8323	0.8088	0.8841	0.8587
2001 Perú	0.8334	0.8575	0.6697	0.7549
2003 Japan	0.7753	0.7838	0.9139	0.9129
2006 Indonesia	0.7483	0.8531	0.8134	0.9030
2007 Solomon Isl.	0.6422	0.7575	0.8412	0.8626
2007 Perú	0.8380	0.8085	0.8872	0.8896
2009 Samoa	0.6987	0.7353	0.7779	0.8093
2010 Chile	0.7346	0.6039	0.8682	0.7820
2011 Japan	0.8571	0.7074	0.9229	0.8311
2012 Canada	0.6829	0.6034	0.8731	0.8398
2014 Chile	0.7833	0.6473	0.9051	0.8341
2015 Chile	0.9103	0.7663	0.9603	0.8686

7. The 2009 Mw 8.1 Samoa Islands Region Earthquake

8. The 2010 Mw 8.8 Maule Earthquake

9. The 2011 Mw 9.0 Tohoku Earthquake

10. The 2012 Mw 7.8 British Columbia Earthquake

11. The 2014 Mw 8.2 Iquique Earthquake

12. The 2015 Mw 8.3 Illapel Earthquake

For each event we apply the methodology described before. By using the W-phase centroid moment tensor, a scaling law, and a elliptic slip distribution the first source is defined. Then, the linear and non-linear tsunami simulations are performed. The resulting runup distributions are decomposed along latitude and longitude, in order to compare both models. The same procedure is repeated but instead considering a FFM solution.

Table 1 shows the correlation of the runup distributions between the code JAGURS and the presented here (the linear method). Table 2 summaries the CPU times for each stage of the process for each simulation. There is a high degree of agreement within a short time.

Detailed figures of the 24 simulations are provided in the supplementary material, where maximum amplitudes, runup distribution and field measurements are displayed.

4 Application to compliment tsunami alert. Case study: The 2015 Illapel Earthquake

The September 16th a 8.3 Mw earthquake took place in the Coquimbo region in Chile (Melgar et al., 2016; Fuentes et al., 2017). The features of the event were optimals for a tsunami generation. The national agencies deployed the protocols for evacuating

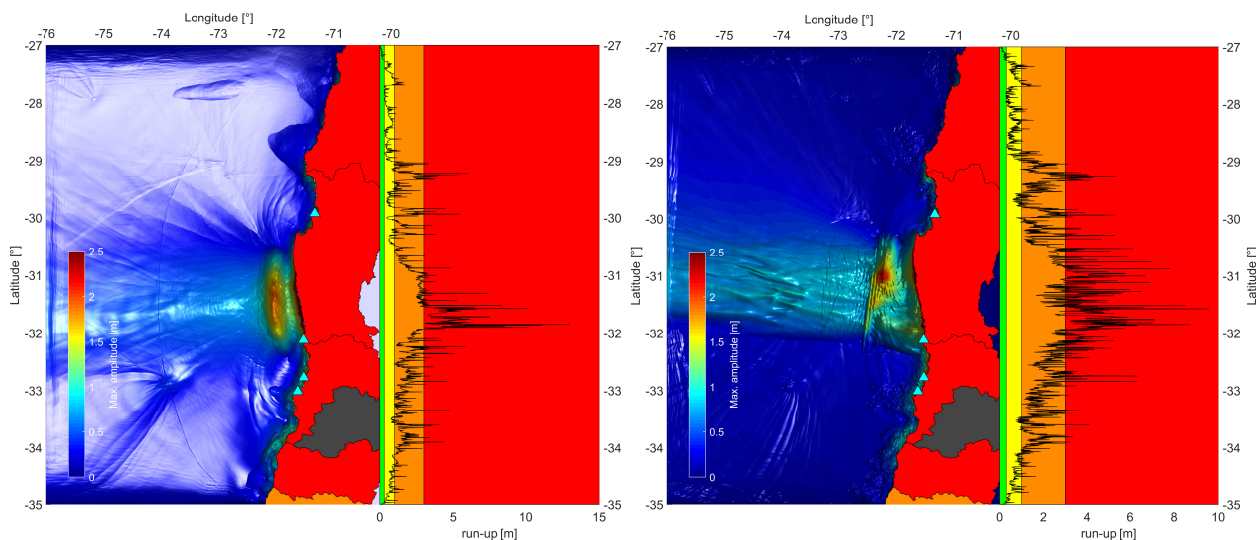Natural Hazards
and Earth System
Sciences
Discussions

Table 2. Results of the CPU time of each event, in seconds. t_{IC} is the time for computing the initial condition, t_{Pr} the time of processing, t_{TP} the time of the tsunami propagation and t_T is the total time.

Event	FFM		Elliptic		LM	JAGURS	Total time t_R			
	t_{IC}	t_{Pr}	t_{IC}	t_{Pr}	t_{TP}	t_{TP}	FFM-LM	FFM-JAGURS	Elliptic-LM	Elliptic-JAGURS
1992 Nicaragua	6	4	8	5	31	575	41	585	44	586
2001 Perú	5	3	7	3	18	360	26	368	28	370
2003 Japan	5	3	9	3	22	428	30	436	34	440
2006 Indonesia	4	3	7	2	20	358	27	365	29	367
2007 Solomon Isl.	8	5	10	5	28	658	41	671	43	673
2007 Perú	4	4	9	4	31	546	39	554	44	559
2009 Samoa	4	3	6	2	17	321	24	328	25	329
2010 Chile	7	4	9	5	32	651	43	662	46	665
2011 Japan	6	6	13	6	46	223	58	235	65	242
2012 Canada	2	1	4	1	15	153	18	156	20	158
2014 Chile	5	4	11	5	24	500	33	509	40	516
2015 Chile	4	4	8	4	27	500	35	508	39	512

the whole chilean coast, even in distant insular territories (SNAM, bulletin #1, Sept. 16th, 23:02 UTC). The decision has to be made the very minutes after the origin time. In general, an accurate prediction of the tsunami runup heights requires a precise image of the seismic source, which nowadays is not available within 5 minutes and worst for real-time by adding the tsunami calculation times. Nevertheless, we can stay close of and quasi real time approach and trigger a first estimation based

5   on the previous elliptical source. Because this can be done in a few seconds, it can be done at the moment instead searching in a precomputed data base of scenarios that are usually restricted. For monitoring purposes, the results can be updated every time a seismic source imaging is received, for both, the near field (at 15 arcsec) and regional field (at 60 arcsec). The whole information is summarized in a coded-color map, following the official coding from the Chilean institutions (Melgar et al., 2016).

10   Color coded maps are self-explicative, which make them easy to interpret (Figures 2 and 3). Each region can be rapidly assigned with a color which deploy an specific protocol for evacuation. All the simulations were performed with two hours of propagation, where the main energy content plays a key role on the inundation process. Figure 4 exhibits the normalized energy rate that generates the runup history along the coast, showing that majority of the global energy is concentrated within the first hour. We can also observe that the first estimation made with the elliptic fault predicts the same levels of inundation as

15   the further finite fault model in the near field, and with minor differences in the regional field. This agrees the common sense where finite fault models act in the monitory stage and time is not as critic as in the very first minutes.

For completeness purposes, travel times isochrones are computed along the pacific basin (Figure 5). This is performed by computing a dense set of rays following Sandanbata et al. (2018), which allows to include dispersive effects. Also, we have

Figure 2. Near Field Simulation of the 2015 Illapel Earthquake for elliptic source (left) and finite fault model (right). Red color represents the run-ups larger than 3 meters. Orange color is between 1 m and 3 m. Yellow color ranges between 0.3 m and 1 m. Green color codes run-ups smaller than 0.3 m.

included the effect of the earth elasticity as shown in An and Liu (2016). This kind of maps can be computed instantly with the very first estimation of the moment tensor and then update.
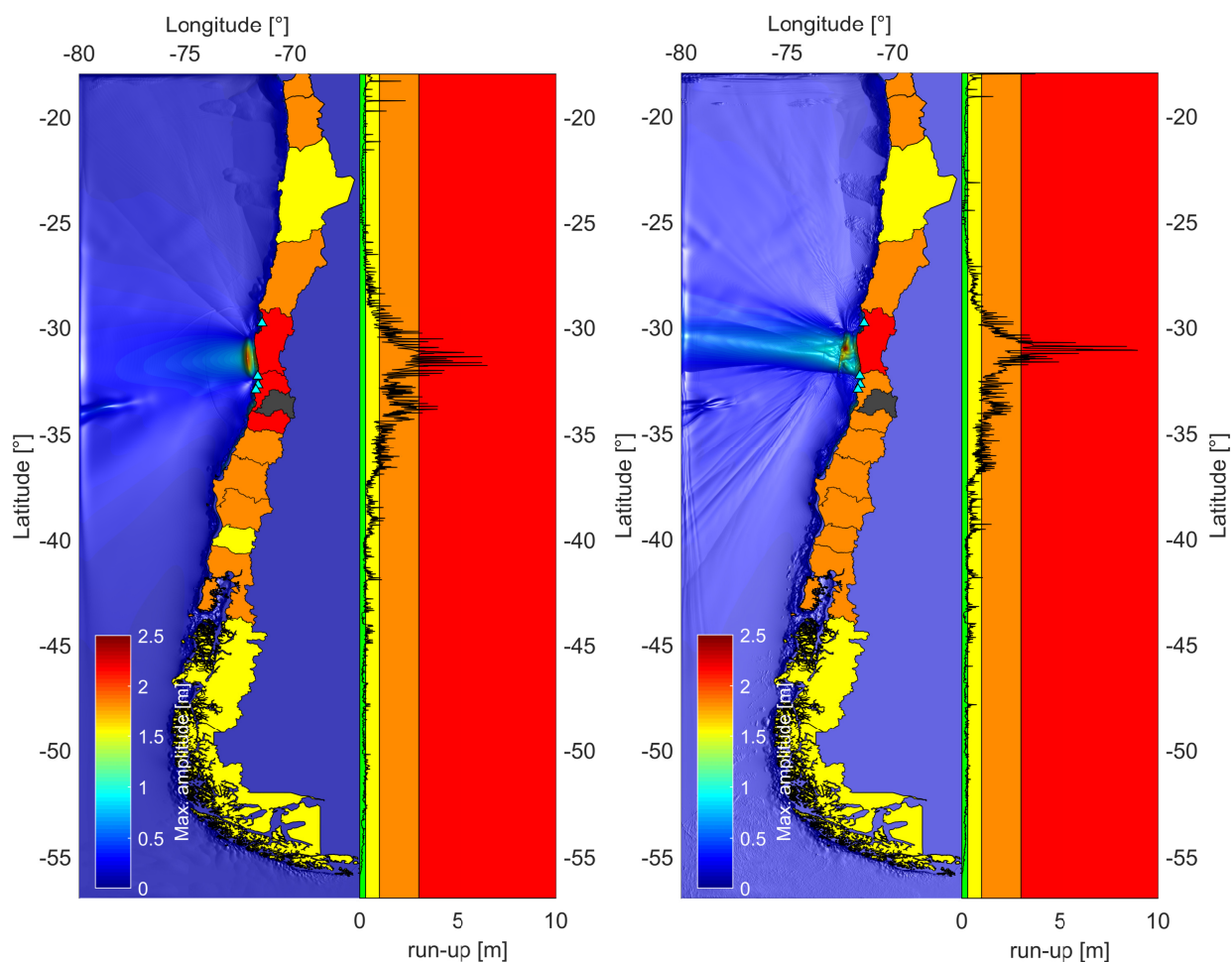
5 Discussion and Conclusions

Despite linear theory has been used in other tsunami warning systems, for instance, in the PTWC (http://unesdoc.unesco.org/
5 images/0022/002203/220368e.pdf), now it is used in combination with more complex sources and faster algorithms with an unique and simple product easy to interpret.

The non-complexity of the source, does not seem to be a problem when it comes to do a fast run-up estimation regarding emergency response. Establishing levels of hazard in real time, tries to generate a more accurate extension of the area affected by the tsunami, the maximum inundation that can reach, and how many people will be exposed to this hazard along the chilean
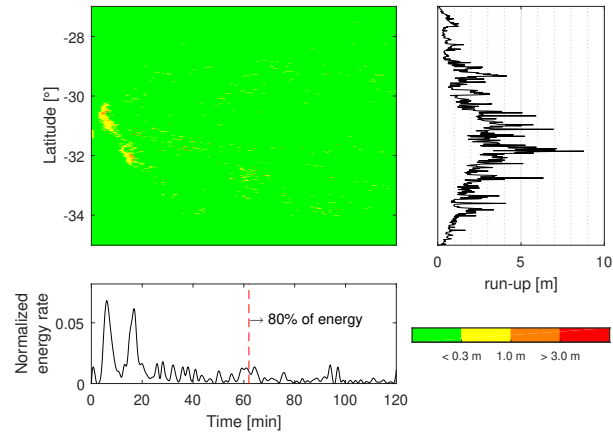10 coast.

This method intends to rapidly predict the run-up distribution. Using some simplifications in the tsunami equations it is possible to model rapidly the observed run-up. Obviously, this is not a high performance computing code, but even with many details outside the modeling such as complexity of the source, fine bathymetry and simplified equations, it can predict an important percentage of the run-up.
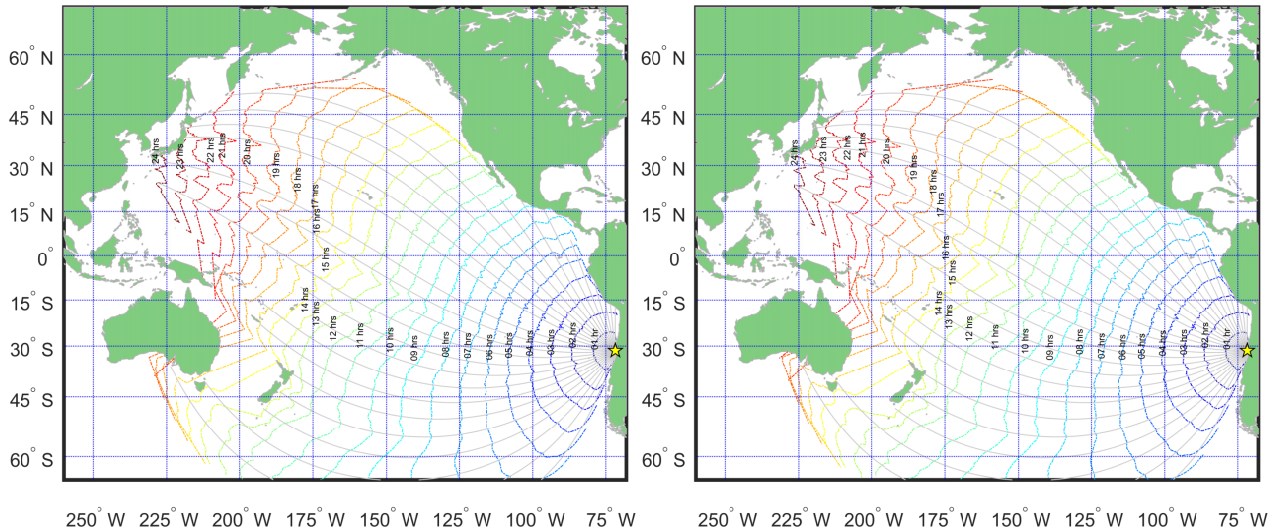
Figure 3. Regional Field Simulation of the 2015 Illapel Earthquake for elliptic source (left) and finite fault model (right). Red color represents the run-ups larger than 3 m. Orange color is between 1 m and 3 m. Yellow color ranges between 0.3 m and 1 m. Green color codes run-ups smaller than 0.3 m.
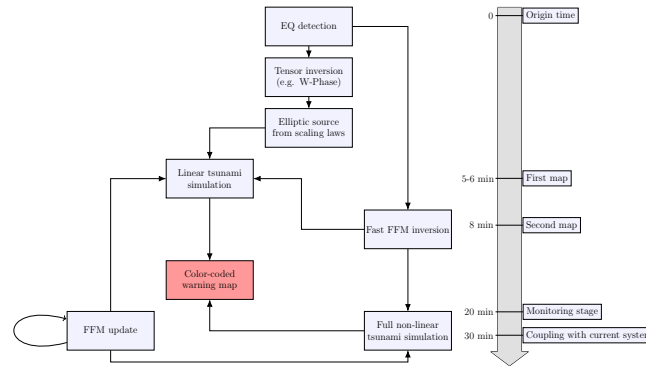
Figure 4. Normalized run-up energy rate during the first two hours of tsunami simulation. Upper left panel display the run-up rate along latitude and time. Upper right panel shows the final maximum run-up and bottom left panel exhibits the normalized energy rate of the whole process as a time series.

Figure 5. Travel times along the pacific basin due to the 2015 Illapel Earthquake. Left panel is purely Shallow Water and right panel includes dispersion and earth elasticity for a wave frequency of 2 mHz.

The idea of extension even without the mathematical rigorosity we would like, is not inexact when we think of the idea of an emergency response system that needs to trigger actions that can save lives and reduce economic losses after the occurrence of a large earthquake.

Natural Hazards
and Earth System
Sciences

Open Access

EGU

Discussions

Figure 6. Flow chart of the proposed methodology.

Using the methodology of Sandabata el al. it is possible to instantaneously calculate the tsunami arrival times from sources generated in the far field. This can also be done using tsunami modeling, however this takes a longer time of calculation then this numerical methodology is accurate enough to calculate tsunami travel times from far field events.

When we compare it with tsunami modeling codes, such as JAGURS, this method includes more than 80% of the predicted
5   run-up in a 15 arcsec bathymetry at least 20 times faster. The main purpose of this study is to produce fast run-up estimations with reasonable accuracy.

The idea here is to compliment the tsunami warning information while full and long calculations are being done (Figure 6). This simple method provide simple and reliable information about the tsunami threat, which allows to entities to take decisions properly.

References

AN, C., AND LIU, P. L.: *Analytical solutions for estimating tsunami propagation speeds*, Coastal Engineering, 117, 44-56, 2016.

BABA, T., TAKAHASHI, N., KANEDA, Y., INAZAWA, Y., KIKKOJIN, M.: *Tsunami Inundation Modeling of the 2011 Tohoku Earthquake Using Three-Dimensional Building Data for Sendai, Miyagi Prefecture, Japan.*, In: Kontar Y., Santiago-Fandiño V., Takahashi T. (eds)
5   Tsunami Events and Lessons Learned. Advances in Natural and Technological Hazards Research, 35. Springer, Dordrecht, 2014.

BECKER, J. J., SANDWELL, D. T., SMITH, W. H. F., BRAUD, J., BINDER, B., DEPNER, J., FABRE, D., FACTOR, J., INGALLS, S., KIM, S-H., LADNER, R.,MARKS, K., NELSON, S., PHARAOH, A., SHARMAN, G., TRIMMER, R., VON ROSENBURG, J., WALLACE G., AND WEATHERALL, P.: *Global bathymetry and elevation data at 30 arc seconds resolution: SRTM30_PLUS*, Marine Geodesy, 32(4), 355-371, 2009.

10 BLASER, L., KRÜGER, F., OHRNBERGER, M., AND SCHERBAUM, F.: *Scaling relations of earthquake source parameter estimates with special focus on subduction environment*, Bulletin of the Seismological Society of America, 100(6), 2914-2926, 2010.

DOI, K.: *Tsunami Warning System in Japan*, In: Zschau J., Küppers A. (eds) Early Warning Systems for Natural Disaster Reduction. Springer, Berlin, Heidelberg, 2003.

DMOWSKA, R., AND RICE, J. R.: *Fracture theory and its seismological applications*, Continuum Theories in Solid Earth Physics, 3, 187-
15   255, 1986.

FUENTES, M., RIQUELME, S., HAYES, G., MEDINA, M., MELGAR, D., VARGAS, G., GONZALEZ, J., AND VILLALOBOS, A.: *A study of the 2015 Mw 8.3 Illapel earthquake and tsunami: Numerical and analytical approaches*, In The Chile-2015 (Illapel) Earthquake and Tsunami, 255-266. Birkhäuser, Cham, 2017.

GEIST, E. L.: *Complex earthquake rupture and local tsunamis*, Journal of Geophysical Research: Solid Earth, 107(B5), 2002.

20 HAYES, G.: *The finite, kinematic rupture properties of great-sized earthquakes since 1990*, Earth and Planetary Science Letters 468, 94-100, 2017.

IDE, S., BEROZA, G. C., SHELLY, D. R., AND UCHIDE, T.: *A scaling law for slow earthquakes*, Nature, 447(7140), 76-79, 2007.

KANAMORI, H., AND RIVERA, L.: *Source inversion of Wphase: speeding up seismic tsunami warning*, Geophysical Journal International, 175(1), 222-238, 2008.

25 MELGAR, D., ALLEN, M., RIQUELME, S., GENG, J., LIANG, C., BRAVO, F., BAEZ, J.C., PARRA, H., BARRIENTOS, S., PENG, F., BOCK, Y., BEVIS, M., CACCAMISE, DANA., VIGNY, C., MORENO, M., AND SMALLEY, R.: *Local tsunami warnings: Perspectives from recent large events.*, Geophysical Research Letters, 43(3), 1109-1117, 2016.

OKADA, Y.: *Surface deformation due to shear and tensile faults in a half-space*, Bulletin of the seismological society of America, 75(4), 1135-1154, 1985.

30 REID, R. O., AND BODINE, B. R.: *Numerical model for storm surges in Galveston Bay*, Journal of the Waterways and harbors Division, 94(1), 33-58, 1968.

RIQUELME, S., FUENTES, M., HAYES, G. P., AND CAMPOS, J.: *A rapid estimation of near-field tsunami runup*, Journal of Geophysical Research: Solid Earth, 120(9), 6487-6500, 2015.

RIQUELME, S., BRAVO, F., MELGAR, D., BENAVENTE, R., GENG, J., BARRIENTOS, S., AND CAMPOS, J.: *W phase source inversion*
35   *using high-rate regional GPS data for large earthquakes*, Geophysical Research Letters, 43(7), 3178-3185, 2016.

RIQUELME, S., MEDINA M., BRAVO, F., BARRIENTOS, S., CAMPOS, J. AND CISTERNAS A.: *W-phase Real Time Implementation and Network Expansion: The Experience in Chile 2012-2017s*, Seismological Research Letters, 89(6), 2237-2248, 2018.

Ruiz, J. A., Fuentes, M., Riquelme, S., Campos, J., and Cisternas, A.: *Numerical simulation of tsunami runup in northern Chile based on non-uniform k-2 slip distributions*, Natural Hazards, 79(2), 1177-1198, 2015.

Satake, K.: *Tsunamis*, In: Lee WHK, Kanamori H, Jennings PC, Kisslinger C (eds) International handbook of earthquake and engineering seismology, vol 81A. Academic, Amsterdam, 437-451, 2002.

5   Tanioka, Y., and Satake, K.: *Tsunami generation by horizontal displacement of ocean bottom*, Geophysical Research Letters, 23(8), 861-864, 1996.

Sandanbata, O., Watada, S., Satake, K., Fukao, Y., Sugioka, H., Ito, A., and Shiobara, H.: *Ray Tracing for Dispersive Tsunamis and Source Amplitude Estimation Based on Green's Law: Application to the 2015 Volcanic Tsunami Earthquake Near Torishima, South of Japan*, Pure and Applied Geophysics, 175(4), 1371-1385, 2018.

10   Wächter, J., Babeyko, A., Fleischer, J., Häner, R., Hammitzsch, M., Kloth, A., and Lendholt, M.: *Development of tsunami early warning systems and future challenges*, Natural Hazards and Earth System Sciences, 12(6), 1923-1935, 2012.